Photoemission of Bi_2Se_3 with Circularly Polarized Light: Probe of Spin Polarization or Means for Spin Manipulation?

J. Sánchez-Barriga,[1] A. Varykhalov,[1] J. Braun,[2] S.-Y. Xu,[3] N. Alidoust,[3] O. Kornilov,[4] J. Minár,[2] K. Hummer,[5] G. Springholz,[6] G. Bauer,[6] R. Schumann,[4] L. V. Yashina,[7] H. Ebert,[2] M. Z. Hasan,[3] and O. Rader[1]

[1]*Helmholtz-Zentrum Berlin, Albert-Einstein-Strasse 15, 12489 Berlin, Germany*
[2]*Department Chemie, Ludwig-Maximilians-Universität München, Butenandtstrasse 5-13, 81377 München, Germany*
[3]*Joseph Henry Laboratory and Department of Physics, Princeton University, Princeton, New Jersey 08544, USA*
[4]*Max-Born-Institut, Max-Born-Strasse 2A, 12489 Berlin, Germany*
[5]*University of Vienna, Faculty of Physics, Computational Materials Physics, Sensengasse 8/12, 1090 Vienna, Austria*
[6]*Institut für Halbleiter und Festkörperphysik, Johannes Kepler Universität, Altenbergerstrasse 69, 4040 Linz, Austria*
[7]*Department of Chemistry, Moscow State University, Leninskie Gory 1/3, 119991 Moscow, Russia*

(Received 21 December 2012; revised manuscript received 30 January 2014; published 24 March 2014)

Topological insulators are characterized by Dirac-cone surface states with electron spins locked perpendicular to their linear momenta. Recent theoretical and experimental work implied that this specific spin texture should enable control of photoelectron spins by circularly polarized light. However, these reports questioned the so far accepted interpretation of spin-resolved photoelectron spectroscopy. We solve this puzzle and show that vacuum ultraviolet photons (50–70 eV) with linear or circular polarization indeed probe the initial-state spin texture of Bi_2Se_3 while circularly polarized 6-eV low-energy photons flip the electron spins out of plane and reverse their spin polarization, with its sign determined by the light helicity. Our photoemission calculations, taking into account the interplay between the varying probing depth, dipole-selection rules, and spin-dependent scattering effects involving initial and final states, explain these findings and reveal proper conditions for light-induced spin manipulation. Our results pave the way for future applications of topological insulators in optospintronic devices.

DOI: 10.1103/PhysRevX.4.011046 Subject Areas: Topological Insulators

I. INTRODUCTION

Since the discovery of three-dimensional topological insulators (TIs), the spin properties of their surface states have been of central importance to the field [1]. Spin-resolved angle-resolved photoemission spectroscopy (SR ARPES) has become the most powerful and the sole tool in systematically revealing the spin polarization of the topological surface states (TSSs) in energy and momentum space. Understanding and utilization of the spin properties of TI materials are believed to be the key to measuring the topological invariances hidden in the bulk electronic wave functions [2] and realizing exotic magnetic-spin physics such as the axion electrodynamics [3,4] or the magnetic monopole [5], as well as future spin-based low-power transistors and devices. While extensive SR-ARPES studies on various TI compounds have successfully identified and confirmed the helical spin texture of the TSSs [6–10], much remains to be addressed regarding the critical response of the measured spin properties to the incident light and its polarizations (electric or magnetic fields).

In spite of the considerable success of SR ARPES, it has been recently challenged by other experimental [11,12] and theoretical [13,14] proposals regarding both the efficiency and the reliability of the SR-ARPES measurements in studying the spin properties of TI surfaces. Part of these proposals involves the interpretation of the circular dichroism in the angular distribution (CDAD) of ARPES as the spin polarization of TSSs [11–13], which, if correct, can significantly improve the efficiency of spin detection. The CDAD effect has also been predicted as an indirect measure of the intrinsic momentum-space orbital-angular-momentum texture of the TSSs [15,16]. These interpretations are, however, unrealistic for several reasons, and one is the dominance of final-state effects in CDAD from TIs that changes sign several times with photon energy [17]. Because of this dominance of final-state effects in an ARPES-based method, the influence of the photoemission process and the significance of conclusions drawn from SR

ARPES of TIs, so far conducted using linearly polarized light, are under question.

On the other hand, in the presence of strong spin-orbit coupling, such a predicted orbital texture would likely be better coupled to and thus easier controlled by electric fields that can be utilized in coherent spin rotation [18], spin-orbit qubits [19], as well as photon-polarization-driven spin-current devices based on the spin-orbit-coupled electrons on TI surfaces [20]. In this context, a recent theoretical work [14] has also raised concerns regarding the reliability of SR ARPES in properly revealing the spin polarization of TSSs, in particular, concerning the response of the measured spin properties to the polarization of the incident light. Assuming strong spin-flip or spin-rotation effects during the photoemission process, it has been proposed that the spin texture of the photoelectrons (i.e., of the final states) is completely different from that of the TSSs in the initial state when linearly or circularly polarized light is used under specific experimental conditions and sample geometries, depending on the angle between light polarization and initial-state spins [14]. Consequently, the measured spin texture of the photoelectrons should completely "lose memory" of the initial-state spin texture and instead rotate depending on the chosen polarization of the incident light. However, it is important to note that the previously existing SR-ARPES data have been interpreted under the assumption that electron spins emitted from TI surfaces are conserved in the photoemission process. Following the first theoretical work [14], a recent SR-ARPES experiment using laser light of 6-eV photon energy [21] has reported spin-resolved data strongly supporting the spin-rotation final-state scenario, and it was concluded that this scenario generally dominates the spin polarization of photoelectrons emitted from TIs [21,22]. While such final-state effects are of high interest for the purpose of spin manipulation in optospintronics applications, these theoretical and experimental studies do, on the other hand, also strongly challenge the reliability and robustness of SR ARPES in studying the spin properties of TI surfaces. Considering the fact that SR ARPES is presently the only available tool for such a purpose, it is critically important to systematically study the impact of such final-state effects in SR-ARPES measurements under different experimental conditions, namely, under which conditions the proposed final-state effects are merely a weak perturbation on the initial spin texture and when they become enhanced or even dominate, as proposed recently [14,21,22].

In the present work, we utilize the TSS of the prototype TI Bi_2Se_3 to systematically investigate the recently proposed basis of manipulating the spin orientation of photoelectrons emitted from the surfaces of TIs by the polarization of the incident photons [14]. By using different experimental conditions and sample geometries, we investigate the reliability of SR ARPES in studying the initial-state spin texture of TSSs with linearly and circularly polarized photons. We demonstrate the existence of two limiting cases where spin manipulation with light polarization is either a weak perturbation or strongly dominates the photoemission process. We further identify the underlying mechanism that triggers the spin polarization and support our experiments by comparing to results of one-step-model photoemission calculations.

II. RESULTS

We perform SR-ARPES measurements on Bi_2Se_3 films with linearly p-polarized and circularly polarized light of opposite helicities ($C+$ and $C-$) incident at an angle of $\phi = 45^\circ$ with respect to the sample normal. Because it is theoretically expected that light-induced manipulation of photoelectron spins must depend on the angle between light polarization and initial-state spin [14], we use two different sample geometries shown in Fig. 1(a) (geometry I) and Fig. 2(a) (geometry II). (For more details, please see Sec. IV and the Supplemental Material [23].) Figure 1 shows SR-ARPES results of the in-plane spin polarization of the TSS and bulk valence-band states of Bi_2Se_3 measured using sample geometry I with different photon energies and light polarizations. In order to investigate the predicted spin-rotation final-state effect [14], we first reverse the helicity of the circular light polarization to search for photon energies where the circular dichroism in ARPES changes its sign. We find for Bi_2Se_3 pronounced sign changes in the CDAD signal between 50 and 70 eV. We note that these photon energies are different from the ones reported for Bi_2Te_3 [17]. Specifically, the color representation of the CDAD asymmetry $A = \frac{I(C+)-I(C-)}{I(C+)+I(C-)}$ (where I is the photoemission intensity) shows that for the upper Dirac cone, it reverses from 50 eV [Fig. 1(b)] to 60 eV [Fig. 1(e)], while for the lower Dirac cone, it reverses from 60 to 70 eV [Fig. 1(h)]. Therefore, we search at these photon energies for coupling to final-state effects in the spin polarization caused by the circular light polarization.

We select a few $\mathbf{k}_\parallel$ wave vectors that are marked by dashed green lines in Figs. 1(b), 1(e), and 1(h). Upon reversal of the circular light polarization, changes (for fixed $\mathbf{k}_\parallel$ and photon energy) are neither observed in the spin-resolved spectra [Figs. 1(c1), 1(c2), 1(f1), 1(f2), 1(i1), and 1(i2)] nor in the corresponding spin polarizations [Figs. 1(d1), 1(d2), 1(g1), 1(g2), 1(j1), and 1(j2)]. In addition, the spectra are indistinguishable from measurements with linear light polarization [symbol $\leftrightarrow$ in Figs. 1(c3) and 1(c4)]. The out-of-plane spin polarization under this sample geometry is found to contribute unobservably to the measured spin polarizations. The fact that the in-plane spin polarization does not change indicates that the circularly polarized light does not align the spins parallel to the surface normal for $C-$ and antiparallel for $C+$ polarization, in spite of what has been predicted [14]. According to Ref. [14], either zero or very small in-plane

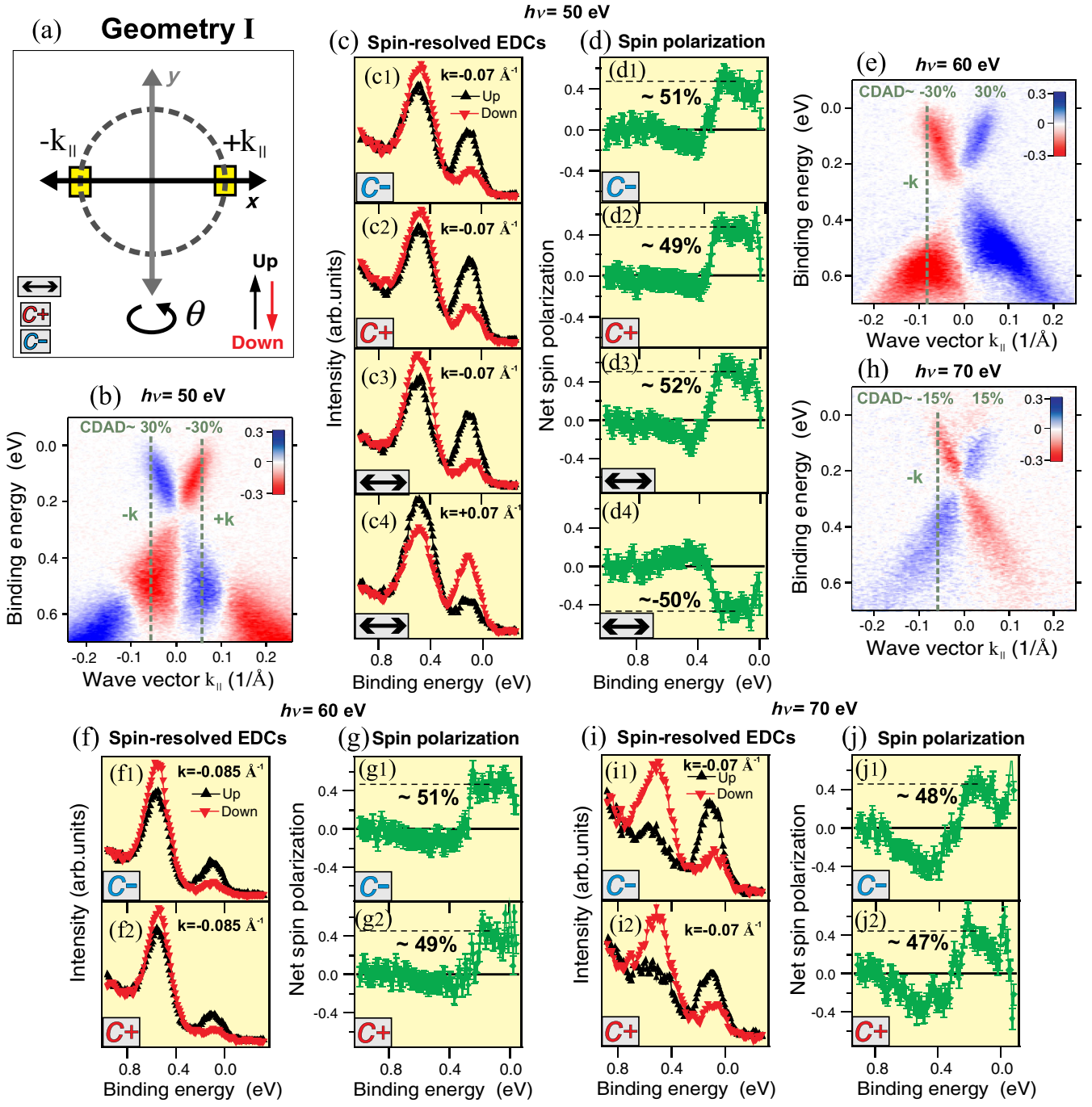

FIG. 1. Observation of the initial-state in-plane spin polarization upon reversal of the CDAD effect from the TSS using (a) geometry I (where the polar angle θ of the sample is rotated), different photon energies and light polarizations [linear ($\leftrightarrow$), circular positive ($C+$), and circular negative ($C-$)]. The dotted circle represents an ideal Dirac cone, and the yellow rectangles represent momentum regions where the SR-ARPES measurements have been taken. (b),(e),(h) $\mathbf{k}$-resolved CDAD asymmetry shown for each photon energy. The dashed green lines on top mark the $\mathbf{k}_\parallel$ wave vectors for which SR-ARPES measurements are presented. The CDAD values from the TSS near the Fermi level are given at the tops. (c),(f),(i) Spin-resolved energy-distribution curves (EDCs) measured for different wave vectors, photon energies, and light polarizations. The black (red) curves show tangential spin-up (down) EDCs. The spin-up (down) direction is denoted by the black (red) arrow in (a). (d),(g),(j) To the right of each spin-resolved EDC, the corresponding net tangential spin polarization is shown and its magnitude indicated.

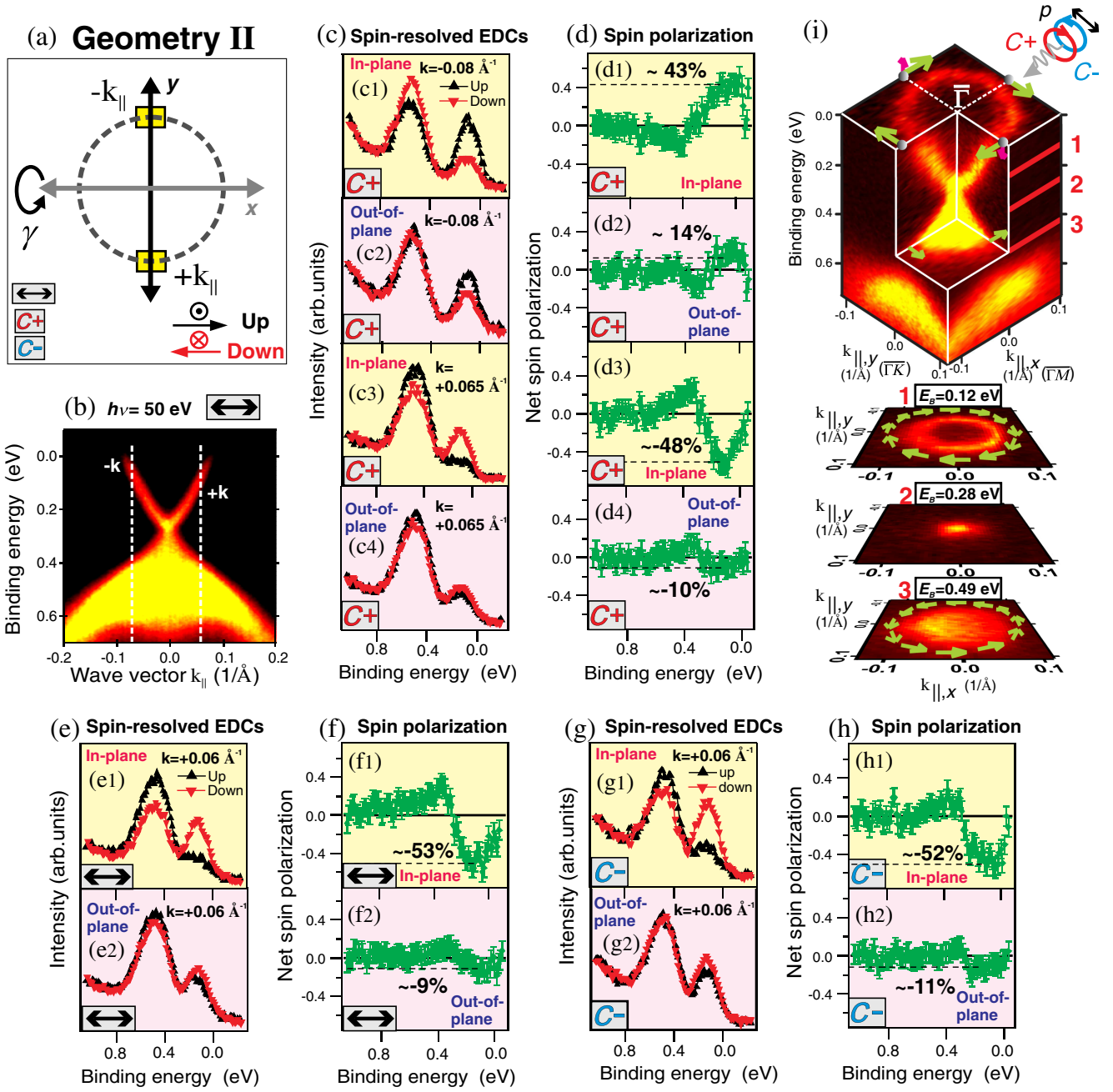

FIG. 2. In-plane and out-of-plane spin polarizations from the TSS measured at 50 eV using (a) geometry II (where the tilt angle γ of the sample is changed) as well as different light polarizations. The dotted circle represents an ideal Dirac cone, and the yellow rectangles represent momentum regions where the SR-ARPES measurements have been taken. (b) ARPES intensity obtained with linear *p*-polarized light. (c),(e),(g) In-plane [(c1),(c3),(e1),(g1)] and out-of-plane [(c2),(c4),(e2),(g2)] spin-resolved EDCs measured for various $\mathbf{k}_\parallel$ wave vectors [marked by dashed white lines in (b)]. The in-plane (out-of-plane) spin direction is given in (a). The red (black) arrow in (a) indicates the in-plane up (down) spin direction, and the black dot (red cross) the spin direction parallel (antiparallel) to the surface normal. (d),(f),(h) To the right of each spin-resolved EDC, the corresponding net spin polarizations are shown. (i) Summary of the results from SR-ARPES measurements at 50 eV. Top: The helical spin texture is probed in four $\mathbf{k}_\parallel$ directions ($\pm\overline{\Gamma K}$ and $\pm\overline{\Gamma M}$). The Fermi surface exhibits a small distortion due to hexagonal warping. The in-plane (green arrows) and out-of-plane (pink arrows) photoelectron spin directions are in vector and magnitude independent of the light polarization. Bottom: Schematics of the observed in-plane helical spin texture superimposed on constant-energy surfaces extracted from the data shown at the top.

spin polarizations would have been expected for $C-$ as well as $C+$ in Fig. 1.

We further demonstrate in Fig. 2 that the coupling to the light polarization is indeed weak by showing SR-ARPES results of the in-plane as well as the out-of-plane spin polarizations measured at 50 eV using sample geometry II. The spin perpendicular to the surface does not reach the predicted 100% but stays small (approximately 10%). This small polarization is not reversed between $C+$ [Fig. 2(d4)] and $C-$ [Fig. 2(h2)] and also does not change when switching from circular to linear light polarization [Fig. 2(f2)]. Instead, the out-of-plane spin polarization reverses with $\mathbf{k}_{\|}$ [Fig. 2(d2)], indicating that it is an initial-state effect. The reason is hexagonal warping [24] near the Fermi surface [see the top of Fig. 2(i)] that is rather small in Bi_2Se_3 as compared to Bi_2Te_3 [8].

Moreover, for linearly polarized light, the angle between linear light polarization and spin should lead to a change of the spin in the final state [14], resulting in a complex in-plane spin texture where the circulation of photoelectron spins around the Fermi surface appears similar to the one followed by a magnetic field in an idealized quadrupole [14,21]. Light polarization and in-plane spins are parallel in geometry II and perpendicular in geometry I, but Fig. 2(f1) shows that the in-plane spin polarization has not changed compared to Fig. 1(d4), demonstrating that it is indeed independent of the sample geometry and follows the expected [7] initial-state helical texture of surface-state electron spins.

The maximum observed in-plane spin polarization in Figs. 1 and 2 is $(50 \pm 10)\%$. This value deviates from recent reports of nearly 100% spin polarization from TSSs in Bi_2Se_3 [9,10]. We do not observe large spin-polarization values at the Dirac point [10] or $\mathbf{k}$-independent spin polarizations contributing to the specific spin texture of TSSs in the photoelectron distribution [10]. Considering

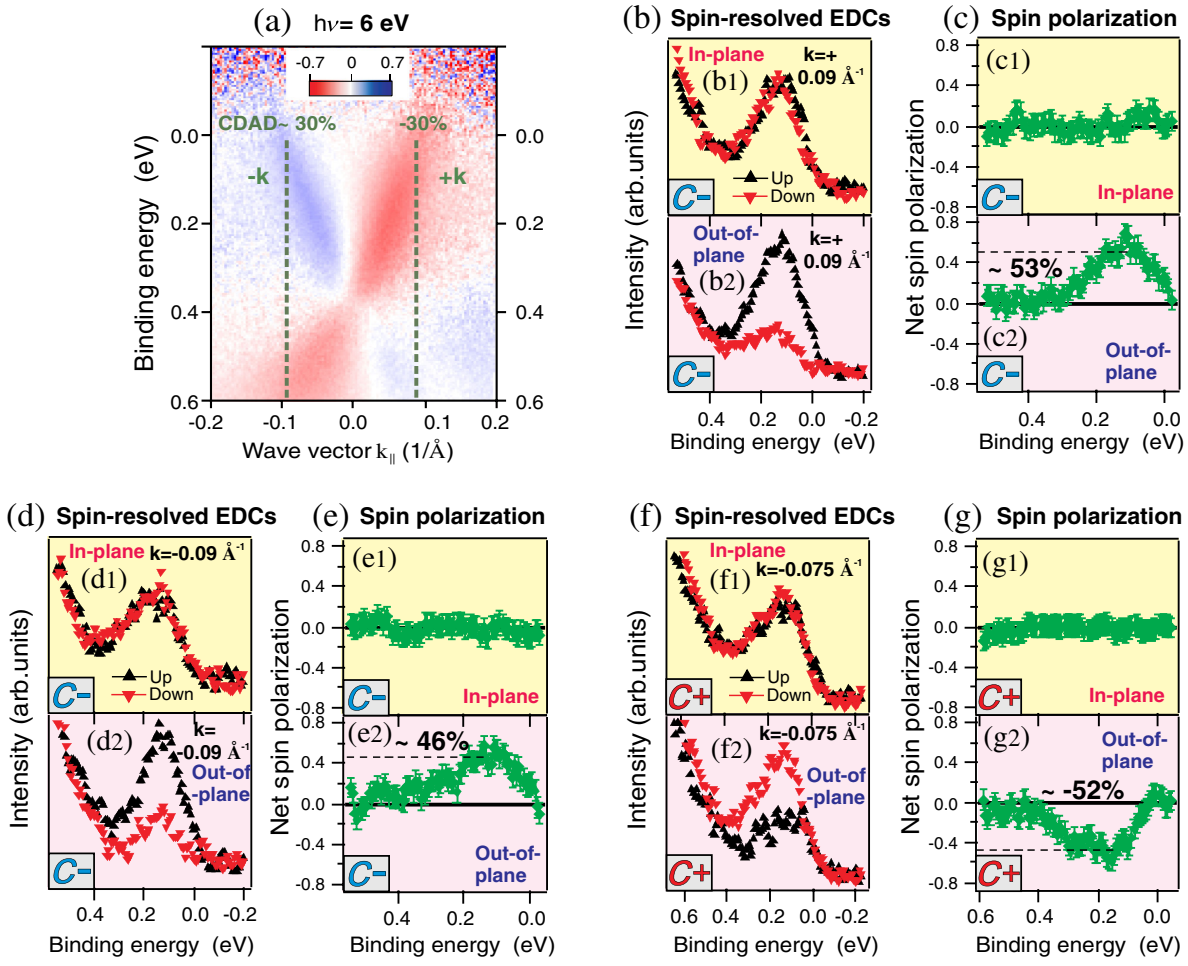

FIG. 3. Out-of-plane switching of the spin texture from the TSS observed upon reversal of the circular light polarization at 6-eV photon energy. (a) $\mathbf{k}$-resolved CDAD asymmetry. The dashed green lines mark the $\mathbf{k}_{\|}$ wave vectors of the SR-ARPES measurements. (b),(d),(f) In-plane [(b1),(d1),(f1)] and out-of-plane [(b2),(d2),(f2)] spin-resolved EDCs. (c),(e),(g) Corresponding net spin polarizations. The out-of-plane spin polarization (zero in plane) does not reverse when going from $+\mathbf{k}_{\|}$ to $-\mathbf{k}_{\|}$ wave vectors and switches with the light helicity. Spectra are acquired using geometry II as well as (b)–(e) circular negative ($C-$) and (f),(g) circular positive ($C+$) light polarizations.

the multiple orbital origin of the Bi_2Se_3 surface states and their multiple contributions to the net spin polarization, a magnitude of about 50%, as reported here, is consistent with first-principles calculations of Bi_2Se_3 [25]. We do note that in Fig. 1, the measured spin-polarization magnitude of the lower Dirac cone at photon energies of 50 and 60 eV appears considerably reduced as compared to that at 70 eV. This difference can be understood based on the superposition of photoemission from the TSS and the bulk valence band, as the bulk bands in Bi_2Se_3 are essentially unpolarized. Hence, at photon energies (effectively $\mathbf{k}_\perp$ values) where the contribution of the bulk valence band is weak (such as 70 eV), we find that the spin polarization measured from the lower Dirac cone accordingly increases up to the expected value [25].

Figure 2(i) summarizes our experimental findings. The helical spin texture of the TSS (bottom), which reverses at the Dirac point, is observed along four $\mathbf{k}_\parallel$ directions ($\pm\overline{\Gamma K}$ and $\pm\overline{\Gamma M}$) (top). The corresponding photoelectron spin polarizations in plane (green arrows) and out of plane (pink arrows) remain unchanged in orientation and magnitude for the different light polarizations ($C+$, $C-$, $\leftrightarrow$). This result does not change over an extended range of incident photon energies (50–70 eV), although the ARPES spectral weight distribution and CDAD signals have changed drastically within the same photon-energy range. Thus, we conclude that at these photon energies, both the direction and magnitude of the measured photoelectron spin polarization remain representative of the initial TSSs and that the theoretically expected photoelectron spin reorientation contributes very little and almost unobservably to the measured spin polarizations.

However, we find a completely different result when using circularly polarized light at 6-eV photon energy, in agreement with recent experimental findings [21]. Our laser SR-ARPES measurements presented in Fig. 3 reveal that circularly polarized photons flip the photoelectron spins perpendicular to the surface and reverse the resulting out-of-plane spin texture with the sense of circular polarization. Specifically, the in-plane component of the spin polarization is nearly zero [upper panels in Figs. 3(b)–3(g)] and the out-of-plane one is as large as 46%–53% [bottom panels in Figs. 3(b)–3(g)], which is comparable to the polarization value of the in-plane component measured at 50–70 eV in Figs. 1 and 2. Moreover, the out-of-plane spin polarization does not reverse when going from $+\mathbf{k}_\parallel$ to $-\mathbf{k}_\parallel$ wave vectors [compare Figs. 3(c2) and 3(e2)], again differently from the behavior at 50–70 eV. This result suggests that light-induced manipulation of the photoelectron spin must depend on the final states reached at different photon energies, a fact that was not considered in previous theoretical models, where so far only spin-degenerate free-electron-like final states have been taken into account.

III. DISCUSSION

To resolve this issue and further explore the origin of these two contrasting experimental findings, we have performed one-step photoemission calculations including spin-dependent transition-matrix elements between initial and final states. Figure 4(a) shows the in-plane and out-of-plane components of the photoelectron spin polarization calculated at 50-eV photon energy upon reversal of the light helicity using a light-incidence angle of $\phi = 45^\circ$. For simplicity, the spin polarization is displayed on a constant-energy surface above the Dirac point, which is of circular shape and not affected by warping. The calculated in-plane photoelectron spin polarization of 57%–63% remains unaffected upon reversal of the circular photon polarization, thus reflecting the initial-state spin texture of the TSS in qualitative agreement with the experimental results in Figs. 1 and 2. We do note that in Fig. 4(a), the out-of-plane spin-switching effect for opposite light helicities contributes with less than 4% spin polarization in the background of the present calculations. (The color representation, which is proportional to the magnitude of the spin polarization, has been magnified in the upper right quadrants corresponding to calculations of the out-of-plane spin polarization.) On the other hand, the higher absolute theoretical values of the in-plane spin polarization as compared to the experiment at this photon energy are most probably due to a theoretical overestimation of the surface contribution (see the Supplemental Material for details [23]).

The fact that in Bi_2Se_3 free-electron final states are not accessible at photon energies of the order of 50–70 eV becomes clear from, e.g., the reversal of the CDAD effect in ARPES (see Fig. 1), which involves transitions from p-type initial states to d-type final states [17,23]. To reach spin-degenerate free-electron final states in a reasonable approximation, much higher photon energies are required. In order to quantitatively compare to recent theoretical findings [14], Fig. 4(b) shows calculations for such conditions (300 eV) in normal incidence, where we find the result that the out-of-plane spin polarization reverses completely with the circular polarization and reaches ideal values of $\pm 100\%$, as theoretically predicted [14]. We point out that the absolute value of the calculated photoelectron spin polarization scales with the light-incidence angle as approximately $|\cos\phi|$. Thus, similar calculations to the ones shown in Fig. 4(b) but under $\phi = 45^\circ$ incidence lead to reduced out-of-plane spin-polarization values of about 70%, whereas the in-plane spin component remains nearly zero [23]. This way, it is surprising that an experiment at 6 eV appears to confirm a theory that invokes free-electron-like final states, as this type of states are not reached at low photon energies. Therefore, we also perform calculations at 6-eV photon energy using a light-incidence angle of $\phi = 45^\circ$, which allows a quantitative comparison to the experimental results in Fig. 3. Our 6-eV calculations shown

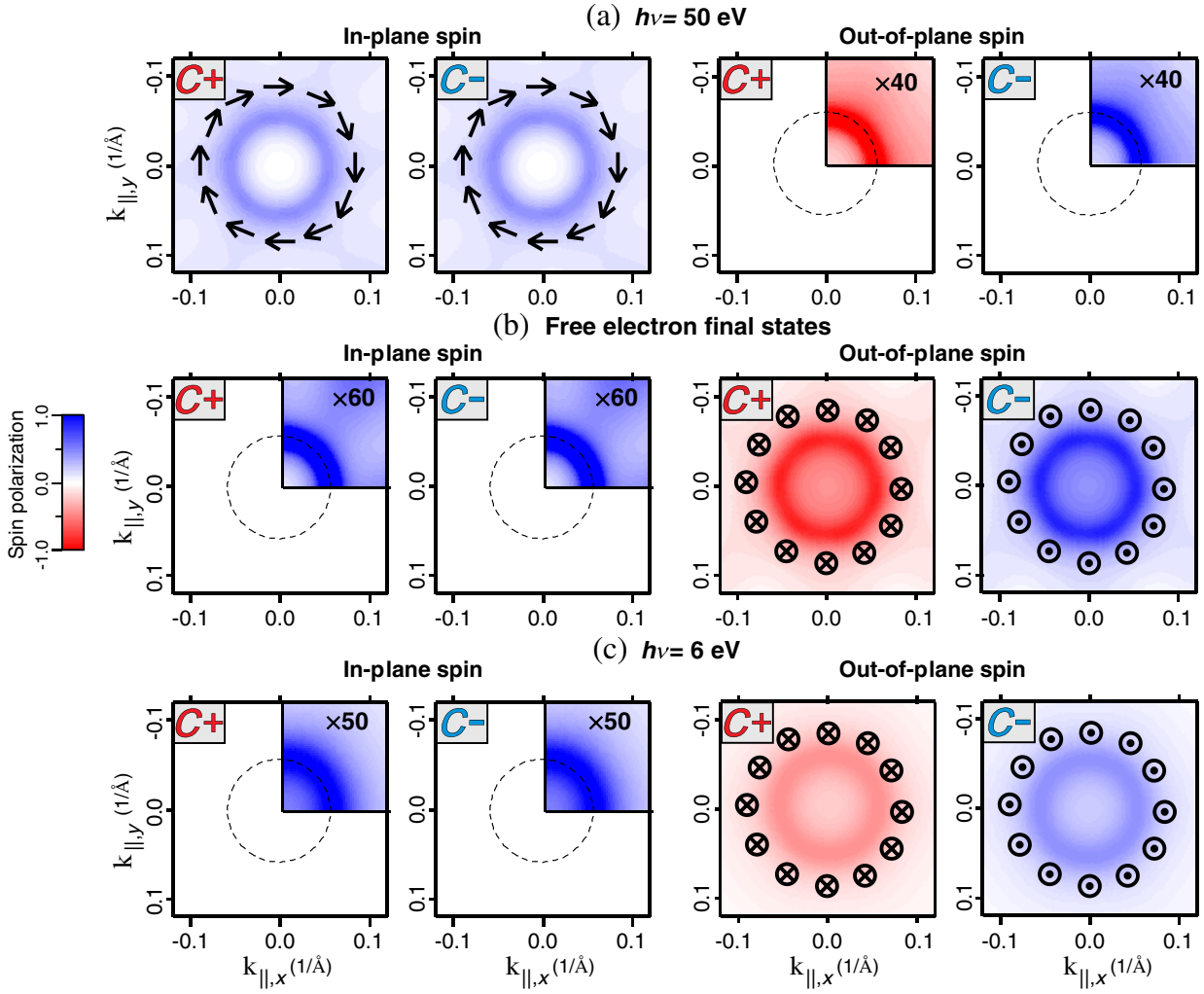

FIG. 4. Calculations of the in-plane (left panels) and out-of-plane (right panels) spin polarization of photoelectrons emitted from the TSS of Bi_2Se_3 upon reversal of the light helicity from $C+$ to $C-$. The spin polarization is displayed on a constant-energy surface of circular shape above the Dirac point. (a) Results at 50 eV under a 45° light-incidence angle, (b) for free-electron-like final states (300 eV) in normal incidence, and (c) at 6 eV again under a 45° light-incidence angle. Arrows in (a) indicate the in-plane spin-polarization directions, dots and crosses in (b) and (c) the spin polarization parallel and antiparallel to the surface normal, respectively. The color intensity is proportional to the magnitude of the spin polarization and has been magnified in the upper right quadrants in those panels where the in-plane [left panels in (b) and (c)] or the out-of-plane [right panels in (a)] spin polarization is nearly zero. Each quadrant is representative of the complete panel, as the results repeat symmetrically about the surface normal.

in Fig. 4(c) reveal that positive and negative circularly polarized photons completely reverse the out-of-plane spin polarization which reaches values of 35%–40%, in qualitative agreement with the free-electron-like final-state calculation in Fig. 4(b) and the experiments in Fig. 3, despite the somewhat smaller absolute values of the spin polarization. The origin of this similarity to the high-energy case is directly linked to dipole-selection rules because 6-eV photon energy enables transitions into s-type final states that are also spin degenerate. Moreover, the final-state wave functions are in both cases the most symmetric ones and are thus connected to the highest symmetry in the atomic case (i.e., an s-like final-state wave function with angular momentum $l = 0$), which is one of the preconditions for optical spin orientation in solid surfaces with circularly polarized light [26]. On the other hand, the smaller calculated values of the out-of-plane and the nearly zero values of the in-plane spin polarization at low photon energies are partially related to the effect of multiple scattering that is fully included in our calculations via spin-dependent scattering-matrix elements [23].

Additionally, one may ask to what extent light-induced spin-polarization control depends on the probing depth of the photoelectrons, which is considered in our theoretical model. The TSS of Bi_2Se_3 extends several layers deep into the bulk (about 2–3 nm) and therefore appears in the spectroscopy for a wide range of probing depths. Indeed, enhanced bulk sensitivity at 6-eV photon energy is

provided by an order-of-magnitude larger probing depth than at 50–70 eV [27], and similarly at photon energies in the x-ray range. Specifically, our detailed analysis of the initial state identifies the low binding-energy states in Bi_2Se_3 as mainly arising from different p orbitals of Bi ($6p^3$) and Se ($4p^4$). Such a contribution from different orbitals results in a layer-dependent spin-orbital texture with a large out-of-plane p_z orbital character within the first quintuple layer (approximately 1 nm), whereas only a relatively small in-plane $p_{x,y}$ contribution is present except for the fifth atomic layer. As a consequence, entanglement between orbital and spin degrees of freedom due to strong spin-orbit coupling is present in our calculations when deeper-lying layers are taken into account, as also reported in recent independent calculations [28]. On the other hand, because the orbital weights decay exponentially with the distance from the surface, the spin polarization at 50–70 eV is dominated by orbital contributions from the first two or three atomic layers, which are predominantly of p_z character. The situation is different for free-electron-like final states and at 6 eV, as the complete first quintuple layer contributes with more or less equal weight to the calculated photoemission intensity. As a result, there is a larger contribution from interference effects between spins originating from different orbitals in the calculated spin-dependent scattering-matrix elements [23]. However, the relative contribution from photoelectron spin interference to the light-induced spin polarization turns out to be a minor one in our calculations. The reason is that manipulation of photoelectron spins with circularly polarized light is ultimately dominated by dipole-selection rules that fully define the orientation of the spin-quantization axis with respect to the surface normal, depending on the incidence angle of the incoming light.

Remarkably, the above results show that we have to distinguish between three different spectral ranges, and this scenario is unambiguously related to the strong influence of the final states reached at different photon energies in the spin-dependent matrix elements. The mechanism underlying this effect originates from the spin dependence of the relativistic dipole matrix elements introduced by the presence of strong spin-orbit coupling. This dependence further implies that in order to populate the final state with a defined spin character depending on the incident light polarization, the final state must be a totally symmetric one. Note that this property is realized in the case of s-like orbitals that transform as the totally symmetric representation [26], fulfilling the requirement of highly symmetric final states, in contrast to d-like final states that are lower in symmetry. An analogous situation is given for free-electron-like final states, which are represented by plane waves. In both cases, relativistic dipole-selection rules unambiguously connect in our calculations the spin character in the final state with a particular excitation channel (see the Supplemental Material for details [23]), revealing proper conditions for light-induced spin manipulation with circularly polarized light. It is only under these specific conditions that the spin polarization of emitted photoelectrons from the TSSs is subject to the effect of optical spin orientation, implying that the spin-quantization axis will be completely parallel to the surface normal when circularly polarized photons are used in normal incidence. This scenario is the case in Fig. 4(b) where, depending on the light helicity, the photoelectron spin polarization points either parallel or antiparallel to the surface normal and exhibits nearly zero in-plane spin components.

Using a photon-incidence angle of $\phi = 45°$, on the other hand, may lead to a rotation of the spin-quantization axis with respect to the surface normal, which means that nonzero contributions in the corresponding in-plane photoelectron spin polarization would be equally expected. However, this result is neither the case in our 6-eV calculations shown in Fig. 4(c) nor in similar calculations performed using free-electron-like final states and circularly polarized photons incident at an angle of 45° [23], as mentioned above. The reason is that in both cases, the magnitude of the calculated in-plane spin-polarization component for opposite light helicities strongly depends on the transition probabilities generated by the z component of the vector potential, which are not present in normal incidence. Specifically, for s-type and free-electron-like final states, these probabilities are relatively small in our calculations. This scenario is further supported by the fact that transitions forbidden in normal emission ($\mathbf{k}_{\parallel} = 0$) contribute with a small weight only, given the small size of the Fermi surface of TSSs (i.e., small nonzero $\mathbf{k}_{\parallel}$ values). Moreover, the scattering potential gradient of the surface layer, which contains a strong spin-orbit contribution, makes the diffraction process of the outgoing photoelectron strongly spin dependent. While this effect plays a less important role in our calculations for free-electron final states [23], for 50–70-eV photons or under the conditions for optical spin manipulation at 6-eV photon energy, it leads to a further reduction of both the in-plane and out-of-plane components of the photoelectron spin polarization, the magnitude of which is subject to the effect of spin-dependent diffraction near the surface.

To summarize, we have experimentally and theoretically investigated the recently proposed suggestion of manipulating the spin polarization of photoelectrons from TIs in SR-ARPES experiments, according to which it should be entirely controlled by the light polarization. For 50–70-eV photons, we have found experimental conditions for which the photoelectron spin polarization measured in SR-ARPES experiments using linear p-polarized and circularly polarized light is the proper probe for the initial-state spin texture of the TSS of Bi_2Se_3. Under these conditions, neither the in-plane nor the out-of-plane spin polarization changes when the polarization of this vacuum ultraviolet light is switched from linear to circular and positive to negative helicity, in full agreement with our one-step

photoemission calculations. In contrast, we have shown that positive and negative circularly polarized 6-eV photons switch the spins perpendicular to the surface, offering manipulation of photoelectron spins with light polarization at this photon energy. Based on our one-step-model calculations, which take into account the interplay between initial and final states, bulk sensitivity, and dipole-selection rules, we have demonstrated that these two contrasting experimental findings are caused by the spin dependence of the relativistic dipole-matrix elements that in turn mainly depend on the final states reached at different photon energies. Our results provide important implications in both understanding and potentially controlling spin degrees of freedom of emitted photoelectrons as well as excited electrons for generating spin currents at TI surfaces using light and its polarizations.

IV. METHODS

SR-ARPES experiments on Bi_2Se_3 films are performed at room temperature in ultrahigh vacuum better than 1×10^{-10} mbar. Experiments at photon energies between 50–70 eV are carried out with polarized undulator radiation at the UE112-PGM1 beam line of BESSY II. The fourth harmonic of a homemade fs laser with central wavelength $\lambda = 800$ nm and a pulse duration of about 150 fs is used to create circularly polarized light of 6-eV photon energy. Spin analysis of the photoelectrons is provided by a Rice University Mott-type spin polarimeter [29] coupled to a Scienta R8000 hemispherical analyzer. The energy resolution of the SR-ARPES experiment is about 80 meV, and the angular resolution is 0.8° [23]. Sample geometries I and II are reached by keeping the rotation about the surface normal (azimuth angle) fixed and rotating either the polar θ or the tilt γ angles of the sample, respectively. Bi_2Se_3 films 400 nm thick are grown by molecular beam epitaxy on $BaF_2(111)$ substrates using a Bi_2Se_3 compound and elemental Se effusion cells. During deposition, the substrate temperature is kept at 360 °C, under which the condition of two-dimensional growth is observed by *in situ* reflection high-energy electron diffraction. Calculations of the SR-ARPES intensity are based on multiple scattering theory within the one-step model of photoemission, including wave-vector, spin-dependent, and energy-dependent transition-matrix elements [30,31]. Initial and final states are obtained for a semi-infinite half-space using the low-energy electron-diffraction method [32]. Further theoretical and experimental details can be found in the Supplemental Material [23].

ACKNOWLEDGMENTS

This work was supported by SPP 1666 of the Deutsche Forschungsgemeinschaft. S.-Y. X., N. A., and M. Z. H. are supported by the Office of Basic Energy Sciences, U.S. Department of Energy (X-Ray Program DOE/BES Grant No. DE-FG-02-05ER46200).

[1] M. Z. Hasan and C. L. Kane, *Colloquium: Topological Insulators*, Rev. Mod. Phys. **82**, 3045 (2010).

[2] C. L. Kane and E. J. Mele, *Z_2 Topological Order and the Quantum Spin Hall Effect*, Phys. Rev. Lett. **95**, 146802 (2005); *Quantum Spin Hall Effect in Graphene*, **95**, 226801 (2005).

[3] A. M. Essin, J. E. Moore, and D. Vanderbilt, *Magnetoelectric Polarizability and Axion Electrodynamics in Crystalline Insulators*, Phys. Rev. Lett. **102**, 146805 (2009).

[4] R. Li, J. Wang, X.-L. Qi, and S.-C. Zhang, *Dynamical Axion Field in Topological Magnetic Insulators*, Nat. Phys. **6**, 284 (2010).

[5] X.-L. Qi, R. Li, J. Zang, and S. C. Zhang, *Inducing a Magnetic Monopole with Topological Surface States*, Science **323**, 1184 (2009).

[6] J. H. Dil, *Spin and Angle Resolved Photoemission on Non-magnetic Low-Dimensional Systems*, J. Phys. Condens. Matter **21**, 403001 (2009).

[7] D. Hsieh, Y. Xia, L. Wray, D. Qian, A. Pal, J. H. Dil, J. Osterwalder, F. Meier, G. Bihlmayer, C. L. Kane, Y. S. Hor, R. J. Cava, and M. Z. Hasan, *Observation of Unconventional Quantum Spin Textures in Topological Insulators*, Science **323**, 919 (2009); D. Hsieh, Y. Xia, D. Qian, L. Wray, J. H. Dil, F. Meier, J. Osterwalder, L. Patthey, J. G. Checkelsky, N. P. Ong, A. V. Fedorov, H. Lin, A. Bansil, D. Grauer, Y. S. Hor, R. J. Cava, and M. Z. Hasan, *A Tunable Topological Insulator in the Spin Helical Dirac Transport Regime*, Nature (London) **460**, 1101 (2009).

[8] S. Souma, K. Kosaka, T. Sato, M. Komatsu, A. Takayama, T. Takahashi, M. Kriener, K. Segawa, and Y. Ando, *Direct Measurement of the Out-of-Plane Spin Texture in the Dirac-Cone Surface State of a Topological Insulator*, Phys. Rev. Lett. **106**, 216803 (2011).

[9] Z.-H. Pan, E. Vescovo, A. V. Fedorov, D. Gardner, Y. S. Lee, S. Chu, G. D. Gu, and T. Valla, *Electronic Structure of the Topological Insulator Bi_2Se_3 Using Angle-Resolved Photoemission Spectroscopy: Evidence for a Nearly Full Surface Spin Polarization*, Phys. Rev. Lett. **106**, 257004 (2011).

[10] Ch. Jozwiak, Y. L. Chen, A. V. Fedorov, J. G. Analytis, C. R. Rotundu, A. K. Schmid, J. D. Denlinger, Y.-D. Chuang, D.-H. Lee, I. R. Fisher, R. J. Birgeneau, Z.-X. Shen, Z. Hussain, and A. Lanzara, *Widespread Spin Polarization Effects in Photoemission from Topological Insulators*, Phys. Rev. B **84**, 165113 (2011).

[11] Y. H. Wang, D. Hsieh, D. Pilon, L. Fu, D. R. Gardner, Y. S. Lee, and N. Gedik, *Observation of a Warped Helical Spin Texture in Bi_2Se_3 from Circular Dichroism Angle-Resolved Photoemission Spectroscopy*, Phys. Rev. Lett. **107**, 207602 (2011).

[12] M. S. Bahramy, P. D. C. King, A. de la Torre, J. Chang, M. Shi, L. Patthey, G. Balakrishnan, Ph. Hofmann, R. Arita, N. Nagaosa, and F. Baumberger, *Emergent Quantum Confinement at Topological Insulator Surfaces*, Nat. Commun. **3**, 1159 (2012).

[13] H. Mirhosseini and J. Henk, *Spin Texture and Circular Dichroism in Photoelectron Spectroscopy from the Topological Insulator Bi_2Te_3: First-Principles Photoemission Calculations*, Phys. Rev. Lett. **109**, 036803 (2012).

[14] C.-H. Park and S. G. Louie, *Spin Polarization of Photoelectrons from Topological Insulators*, Phys. Rev. Lett. **109**, 097601 (2012).

[15] W. Jung, Y. Kim, B. Kim, Y. Koh, C. Kim, M. Matsunami, S. Kimura, M. Arita, K. Shimada, J. H. Han, J. Kim, B. Cho, and C. Kim, *Warping Effects in the Band and Angular-Momentum Structures of the Topological Insulator* Bi_2Te_3, Phys. Rev. B **84**, 245435 (2011).

[16] S. R. Park, J. Han, C. Kim, Y. Y. Koh, Ch. Kim, H. Lee, H. J. Choi, J. H. Han, K. D. Lee, N. J. Hur, M. Arita, K. Shimada, H. Namatame, and M. Taniguchi, *Chiral Orbital-Angular Momentum in the Surface States of* Bi_2Se_3, Phys. Rev. Lett. **108**, 046805 (2012).

[17] M. R. Scholz, J. Sánchez-Barriga, J. Braun, D. Marchenko, A. Varykhalov, M. Lindroos, Y. J. Wang, H. Lin, A. Bansil, J. Minár, H. Ebert, A. Volykhov, L. V. Yashina, and O. Rader, *Reversal of the Circular Dichroism in Angle-Resolved Photoemission from* Bi_2Te_3, Phys. Rev. Lett. **110**, 216801 (2013).

[18] K. C. Nowack, F. H. L. Koppens, Yu. V. Nazarov, and L. M. K. Vandersypen, *Coherent Control of a Single Electron Spin with Electric Fields*, Science **318**, 1430 (2007).

[19] S. Nadj-Perge, S. M. Frolov, E. P. A. M. Bakkers, and L. P. Kouwenhoven, *Spin Orbit Qubit in a Semiconductor Nanowire*, Nature (London) **468**, 1084 (2010).

[20] J. W. McIver, D. Hsieh, H. Steinberg, P. Jarillo-Herrero, and N. Gedik, *Control over Topological Insulator Photocurrents with Light Polarization*, Nat. Nanotechnol. **7**, 96 (2012).

[21] Ch. Jozwiak, C.-H. Park, K. Gotlieb, C. Hwang, D.-H. Lee, S. G. Louie, J. D. Denlinger, C. R. Rotundu, R. J. Birgeneau, Z. Hussain, and A. Lanzara, *Photoelectron Spin-Flipping and Texture Manipulation in a Topological Insulator*, Nat. Phys. **9**, 293 (2013).

[22] Q.-K. Xue, *Full Spin Ahead for Photoelectrons*, Nat. Phys. **9**, 265 (2013).

[23] See Supplemental Material at http://link.aps.org/supplemental/10.1103/PhysRevX.4.011046 for more details.

[24] L. Fu, *Hexagonal Warping Effects in the Surface States of the Topological Insulator* Bi_2Te_3, Phys. Rev. Lett. **103**, 266801 (2009).

[25] O. V. Yazyev, J. E. Moore, and S. G. Louie, *Spin Polarization and Transport of Surface States in the Topological Insulators* Bi_2Se_3 *and* Bi_2Te_3 *from First Principles*, Phys. Rev. Lett. **105**, 266806 (2010).

[26] C. M. Schneider and J. Kirschner, *Spin- and Angle-Resolved Photoelectron Spectroscopy from Solid Surfaces with Circularly Polarized Light*, Crit. Rev. Solid State Mater. Sci. **20**, 179 (1995).

[27] J. D. Koralek, J. F. Douglas, N. C. Plumb, J. D. Griffith, S. T. Cundiff, H. C. Kapteyn, M. M. Murnane, and D. S. Dessau, *Experimental Setup for Low-Energy Laser-Based Angle Resolved Photoemission Spectroscopy*, Rev. Sci. Instrum. **78**, 053905 (2007).

[28] Z.-H. Zhu, C. N. Veenstra, G. Levy, A. Ubaldini, P. Syers, N. P. Butch, J. Paglione, M. W. Haverkort, I. S. Elfimov, and A. Damascelli, *Layer-by-Layer Entangled Spin-Orbital Texture of the Topological Surface State in* Bi_2Se_3, Phys. Rev. Lett. **110**, 216401 (2013).

[29] G. C. Burnett, T. J. Monroe, and F. N. Dunning, *High-Efficiency Retarding-Potential Mott Polarization Analyzer*, Rev. Sci. Instrum. **65**, 1893 (1994).

[30] J. F. L. Hopkinson, J. B. Pendry, and D. J. Titterington, *Calculation of Photoemission Spectra for Surfaces of Solids*, Comput. Phys. Commun. **19**, 69 (1980).

[31] J. Braun, *The Theory of Angle-Resolved Ultraviolet Photoemission and Its Applications to Ordered Materials*, Rep. Prog. Phys. **59**, 1267 (1996).

[32] A. X. Gray, C. Papp, S. Ueda, B. Balke, Y. Yamashita, L. Plucinski, J. Minár, J. Braun, E. R. Ylvisaker, C. M. Schneider, W. E. Pickett, H. Ebert, K. Kobayashi, and C. S. Fadley, *Probing Bulk Electronic Structure with Hard X-Ray Angle-Resolved Photoemission*, Nat. Mater. **10**, 759 (2011).